Chapter V: Results and discussion: $[Cr_3O(Cl_3CCO_2)_6.2H_2O)]Cl_3CCO_2.3H_2O$ as Ziegler-Natta catalyst for ethylene polymerization

5.1 Introduction

The $[Cr_3O(Cl_3CCO_2)_6.2H_2O]Cl_3CCO_2.3H_2O$ complex has been synthesized by treating $CrCl_3.6H_2O$ with trichloroacetic acid. Its single crystal X-ray structure analysis has been published [1] and full characterization of its properties has been described in Chapter II. The complex, a fine green powder, was stable at ambient atmosphere and contained 11.32 % of chromium, (11.30 % theoretical value of chromium content).

The above complex, combined with $AlEt_2Cl$, has been investigated as a potential catalytic system for ethylene polymerization. This chapter describes the effect of varying the monomer pressure on the homopolymerization of ethylene under similar conditions.

Details of materials used, experimental set-up, polymerization procedure and polymer characterization have been described in Chapter III.

A series of polymerization experiments were carried out at constant Al / Cr molar ratio of 45 and 0.08 g of ground chromium complex. The mixture of the μ_3-oxo centered trinuclear chromium(III) carboxylate complex and $AlEt_2Cl$ in toluene was a yellow, heterogeneous solution, with green suspension of finely dispersed chromium compound. The total polymerization solution volume was 400 mL. The catalyst was aged for 40 minutes and each polymerization was carried out at 40 ^oC for one hour using the experimental apparatus detailed in Chapter III.

5.2 Kinetics of ethylene polymerization

Homopolymerization of ethylene was carried out with an initial monomer pressure of 672 kPa using the heterogeneous catalytic system, $[Cr_3O(Cl_3CCO_2)_6.2H_2O]Cl_3CCO_2.3H_2O$ / $AlEt_2Cl$.

Figures 5.1 and 5.2 show, the drop in monomer pressure and in ln P in function of reaction time respectively. As one can observe, for the initial six minutes of the polymerization, the drop in pressure is linear (Figure 5.1). Moreover, the plot of ln P versus reaction time is also linear. These indicate that the polymerization is of first order with respect to monomer [2].

The amount of polyethylene formed under different reaction times in the above experiment is given in Figure 5.3. The fairly linear portion seen in the curve from 21 to 48 minutes indicates that the number of active sites of the catalyst remain constant in that period of time [3].

Figure 5.4 is a representative kinetic curve for ethylene polymerization obtained using the $[Cr_3O(Cl_3CCO_2)_6.2H_2O]Cl_3CCO_2.3H_2O$ / $AlEt_2Cl$ catalytic system with 672 kPa as initial monomer pressure. It is observed that the rate of the polymerization increases sharply to a maximum during the first minute of the polymerization. Then, it decreases to a constant value. As explained earlier (Chapter IV), this decaying-rate behavior is the result of the rapid reaction between the monomer and the active centers at the beginning of the polymerization, followed by deactivating of some of the active sites, resulting in the decrease in the rate of polymerization.

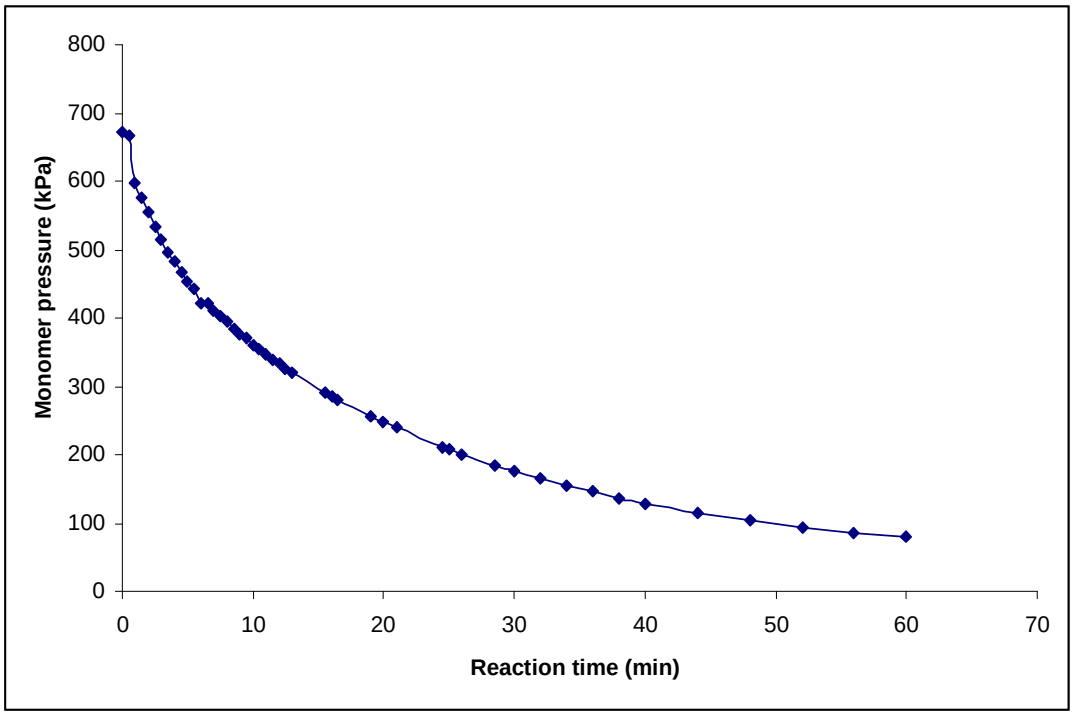

Figure 5.1: Homopolymerization of ethylene with initial monomer pressure of 672 kPa, using $[Cr_3O(Cl_3CCO_2)_6.2H_2O]Cl_3CCO_2.3H_2O$ / $AlEt_2Cl$ catalytic system, Al / Cr = 45

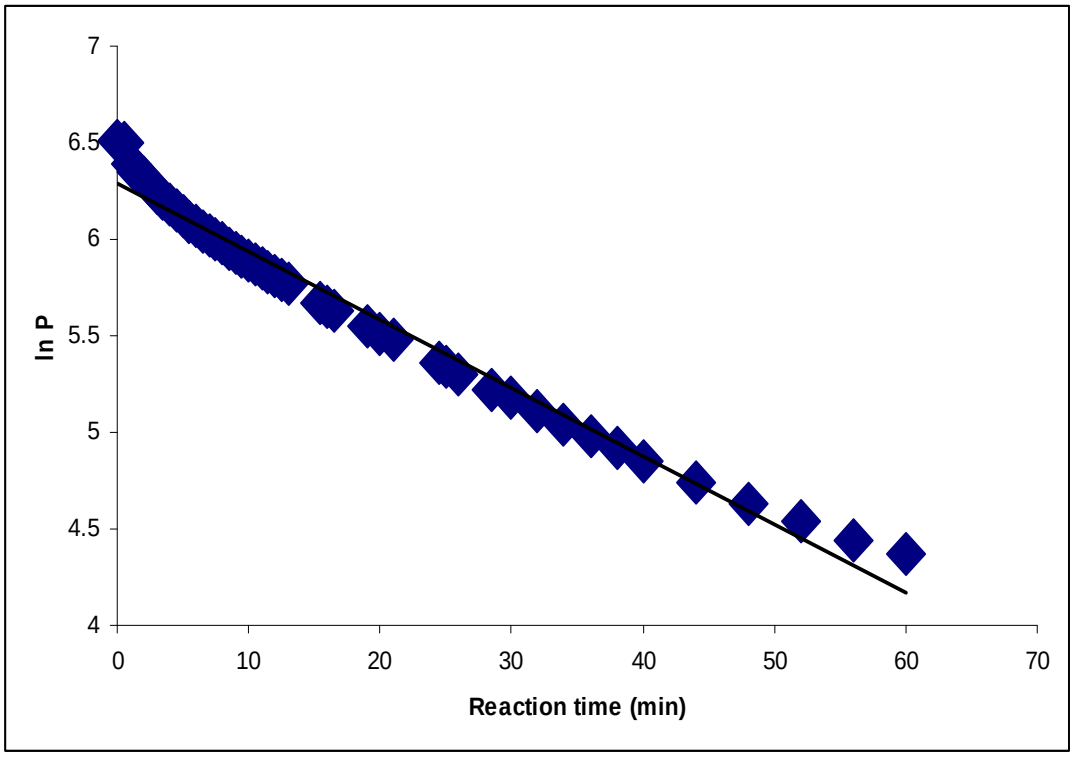

Figure 5.2: Plot of ln P as a function of reaction time for the polymerization of ethylene

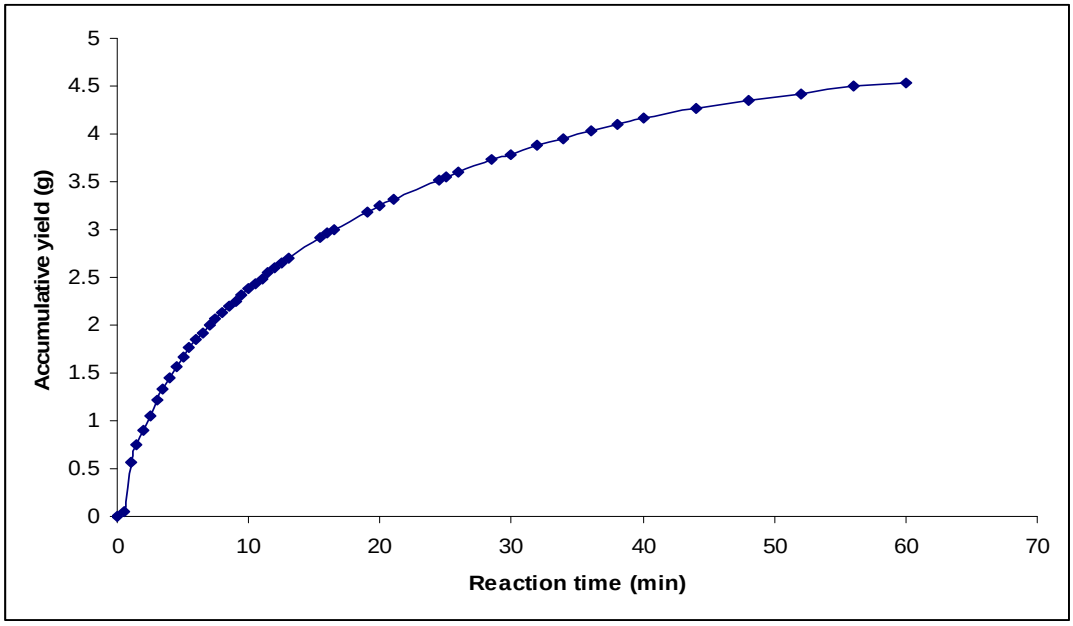

Figure 5.3: Accumulative polymer yield as a function of reaction time, using $[Cr_3O(Cl_3CCO_2)_6.2H_2O]Cl_3CCO_2.3H_2O$ / $AlEt_2Cl$ catalytic system with initial monomer pressure of 672 kPa, Al / Cr = 45, reaction temperature = 40°C, aging time = 40 minutes.

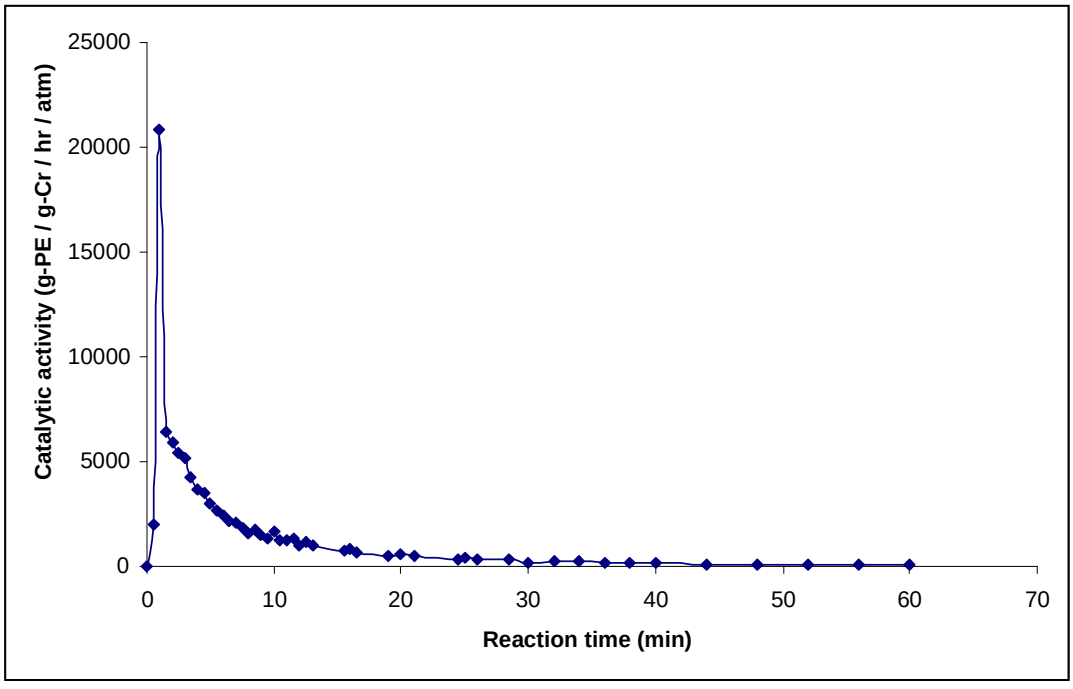

Figure 5.4: Kinetic curve for ethylene polymerization, using $[Cr_3O(Cl_3CCO_2)_6.2H_2O]Cl_3CCO_2.3H_2O$ / $AlEt_2Cl$ catalytic system with initial monomer pressure of 672 kPa, Al / Cr = 45, reaction temperature = 40°C, aging time = 40 minutes.

5.3 Effect of monomer pressure

A series of polymerization experiments were carried out at constant Al / Cr molar ratio of 45 and 0.08 g of ground $[Cr_3O(Cl_3CCO_2)_6.2H_2O]Cl_3CCO_2.3H_2O$ complex. The co-catalyst used was $AlEt_2Cl$ and the medium of the polymerization was toluene. The total polymerization solution volume was 400 mL. The catalyst was aged for 40 minutes and the polymerization was carried out at 40 ^oC for one hour. Table 5.1 summarizes the results obtained from the experiments. As observed, the polymer yield and catalytic activity increase with increase in monomer pressure from 317 kPa to 795 kPa. The highest activity obtained is 36.71 kg-PE / g-Cr / hr / atm at 795 kPa. Figure 5.5 shows the effect of different monomer pressures on the amount of PE produced. In addition, a plot of accumulated yield as a function of time is represent in Figure 5.6. Figure 5.7 shows the effect of initial monomer pressure on the maximum initial activity.

Table 5.1: Catalyst activity and polymer yield at various initial monomer pressures

Run	Initial monomer pressure (kPa)	Maximum initial activity (kg-PE / g-Cr / hr / atm)	Yield (g)
1	317	5.13	2.40
2	412	7.63	2.68
3	505	17.03	3.15
4	672	20.82	4.54
5	795	36.71	5.32

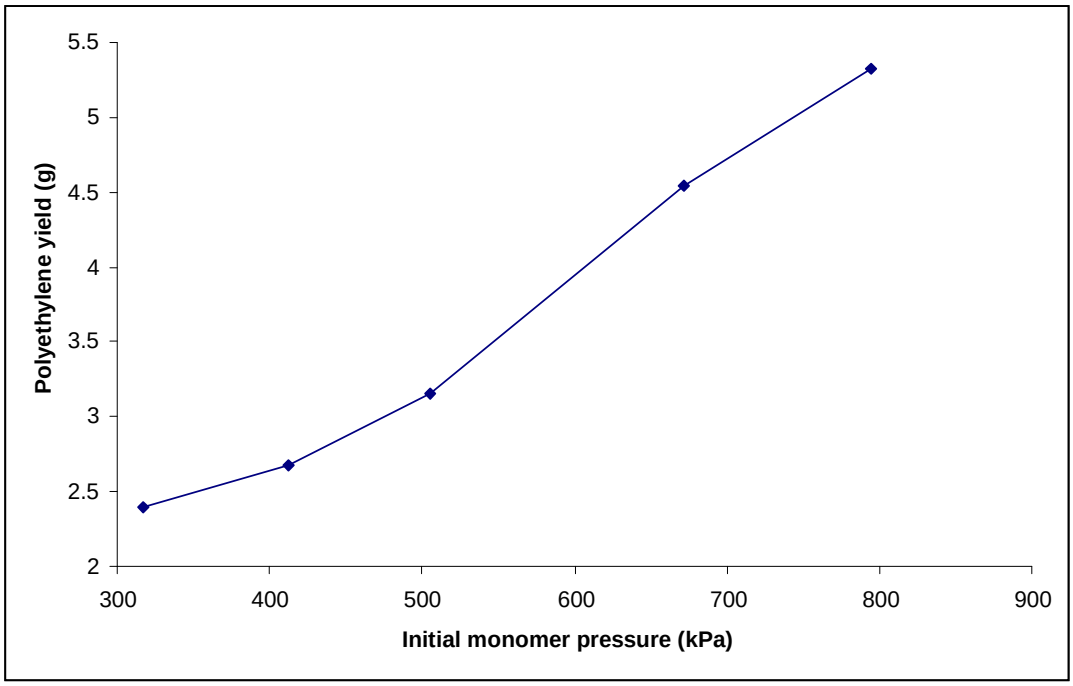

Figure 5.5: Polyethylene yield versus initial monomer pressure, using $[Cr_3O(Cl_3CCO_2)_6.2H_2O]Cl_3CCO_2.3H_2O$ / $AlEt_2Cl$ catalytic system, Al / Cr = 45, reaction temperature = 40 ^oC, aging time = 40 minutes

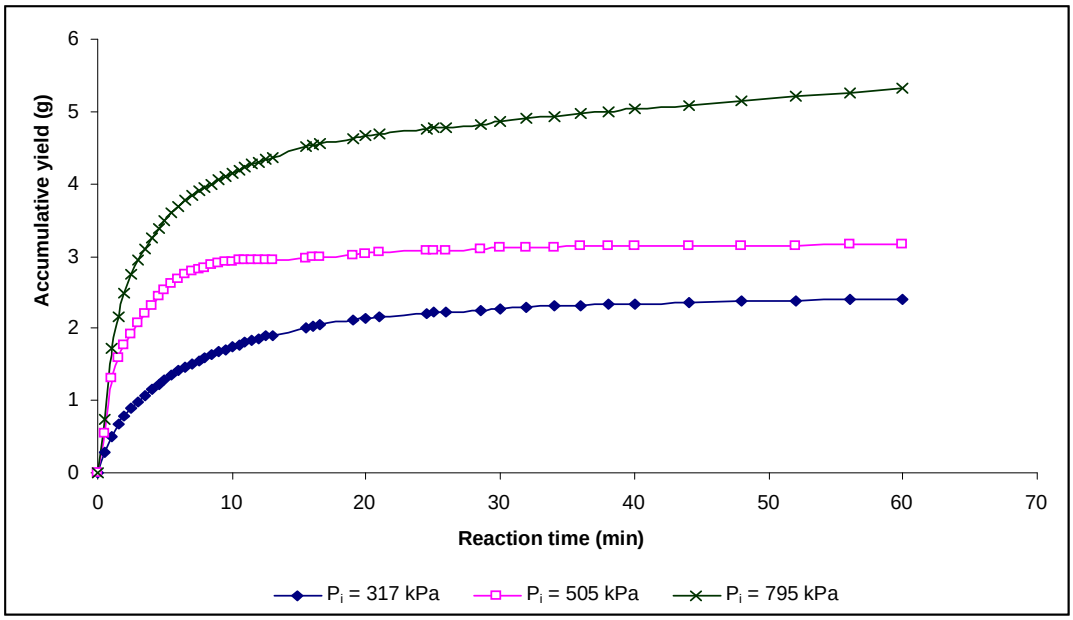

Figure 5.6: Accumulative yield versus reaction time, at various ethylene pressures using $[Cr_3O(Cl_3CCO_2)_6.2H_2O]Cl_3CCO_2.3H_2O$ / $AlEt_2Cl$ catalytic system, Al / Cr of 45, reaction temperature = 40 ^oC, aging time = 40 min

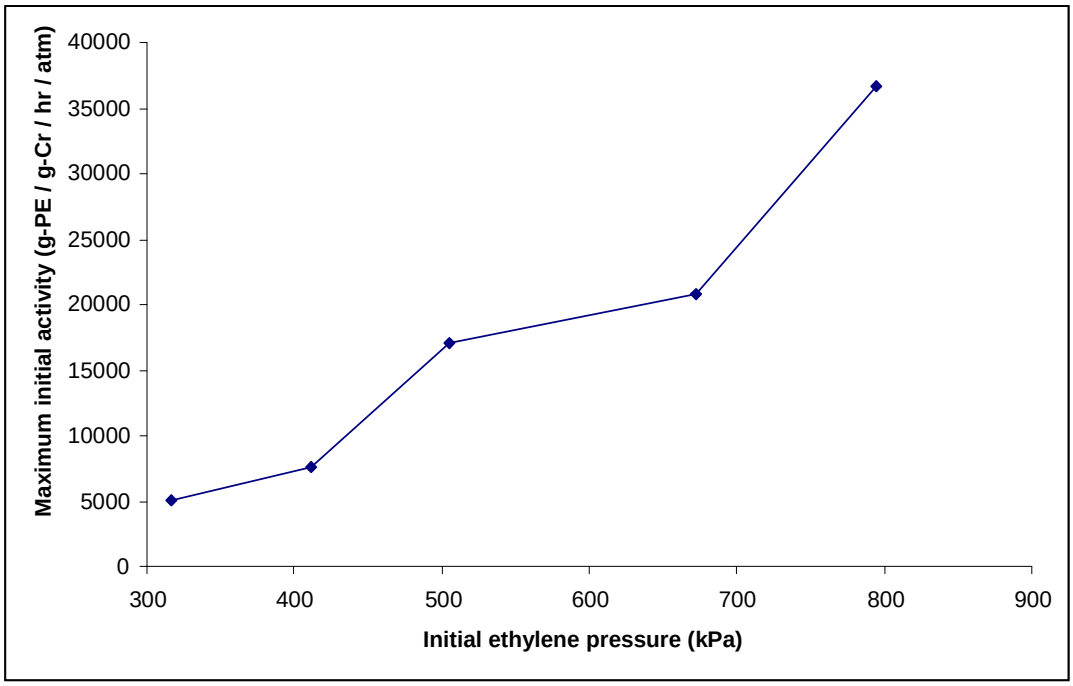

Figure 5.7: Maximum initial activity versus initial monomer pressure, using $[Cr_3O(Cl_3CCO_2)_6.2H_2O]Cl_3CCO_2.3H_2O$ / $AlEt_2Cl$ catalytic system, Al / Cr = 45, reaction temperature = 40 ^oC, aging time = 40 min

The rates of the ethylene polymerization as represented in Figures 5.8 and 5.9 show decay type, similar to those of highly active Ziegler-Natta catalysts [4-6]. The steady state in each experiment was observed during the period of 21 to 48 minutes of the reaction. The polymerization rate initially increases to a maximum in the first minute of the polymerization; then, it decreases abruptly to a steady state, followed by a gradual decline in rate at the end of the polymerization.

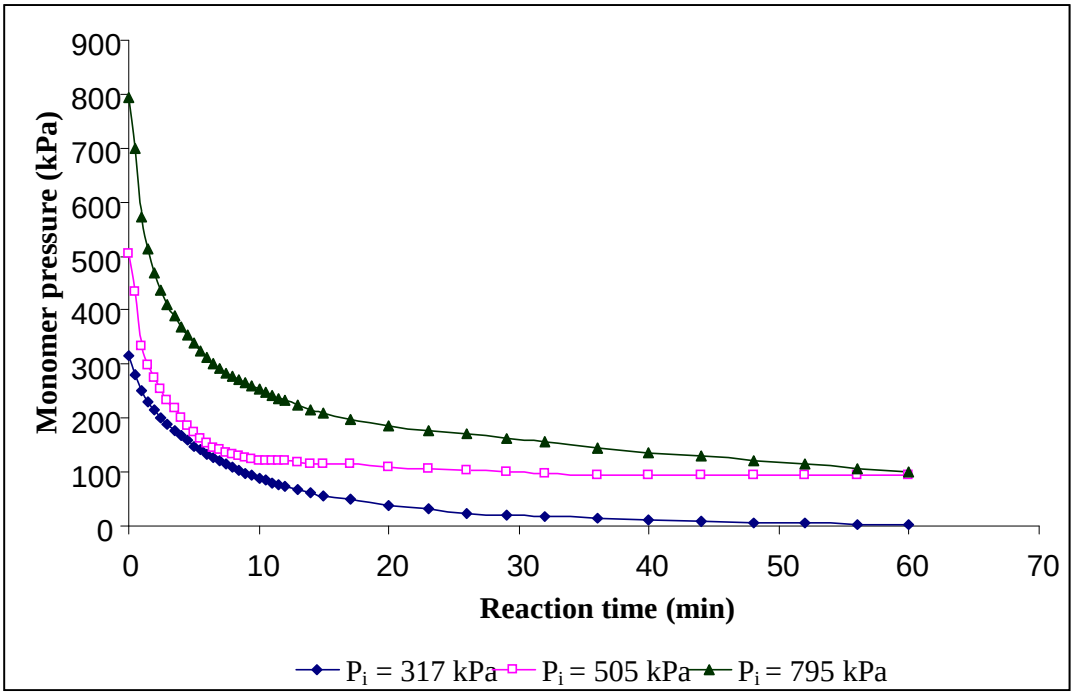

Figure 5.8: Drop in ethylene pressure versus reaction time, at various pressures, using $[Cr_3O(Cl_3CCO_2)_6.2H_2O]Cl_3CCO_2.3H_2O$ / $AlEt_2Cl$ catalytic system, Al / Cr = 45, reaction temperature = 40 ^oC, aging time = 40 min

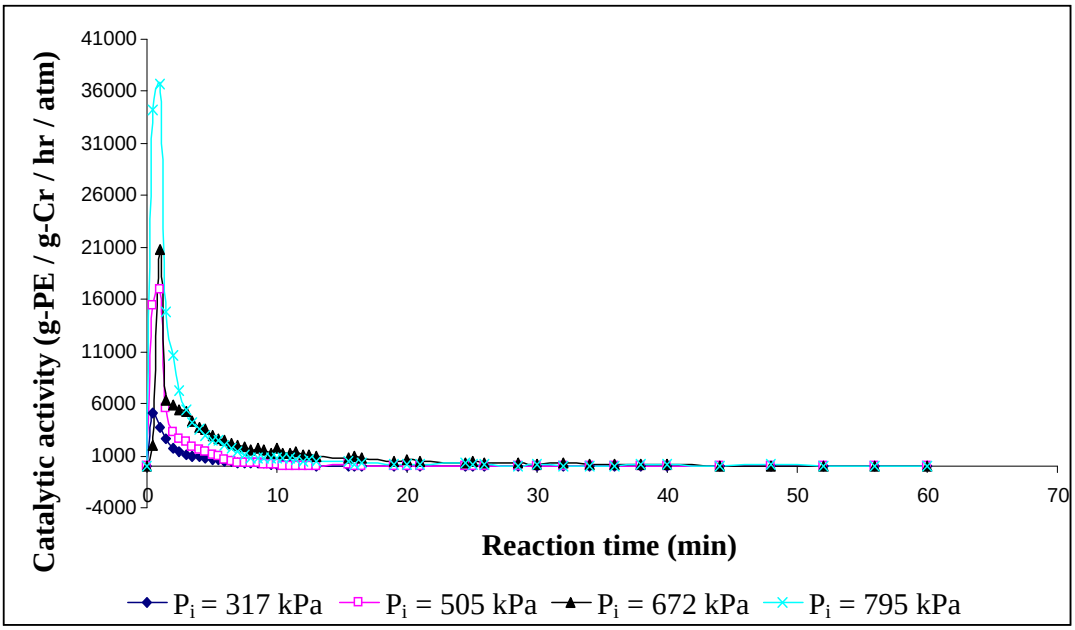

Figure 5.9: Kinetic curves for ethylene polymerization, at various monomer pressures, using $[Cr_3O(Cl_3CCO_2)_6.2H_2O]Cl_3CCO_2.3H_2O$ / $AlEt_2Cl$ catalytic system, Al / Cr of 45, reaction temperature = 40 ^oC, aging time = 40 minutes.

5.4 Characterization of polymers

5.4.1 Morphology

Polyethylene obtained from $[Cr_3O(Cl_3CCO_2)_6.2H_2O]Cl_3CCO_2.3H_2O$ / $AlEt_2Cl$ catalytic system were white and clumpy particles as seen in Figure 5.10.

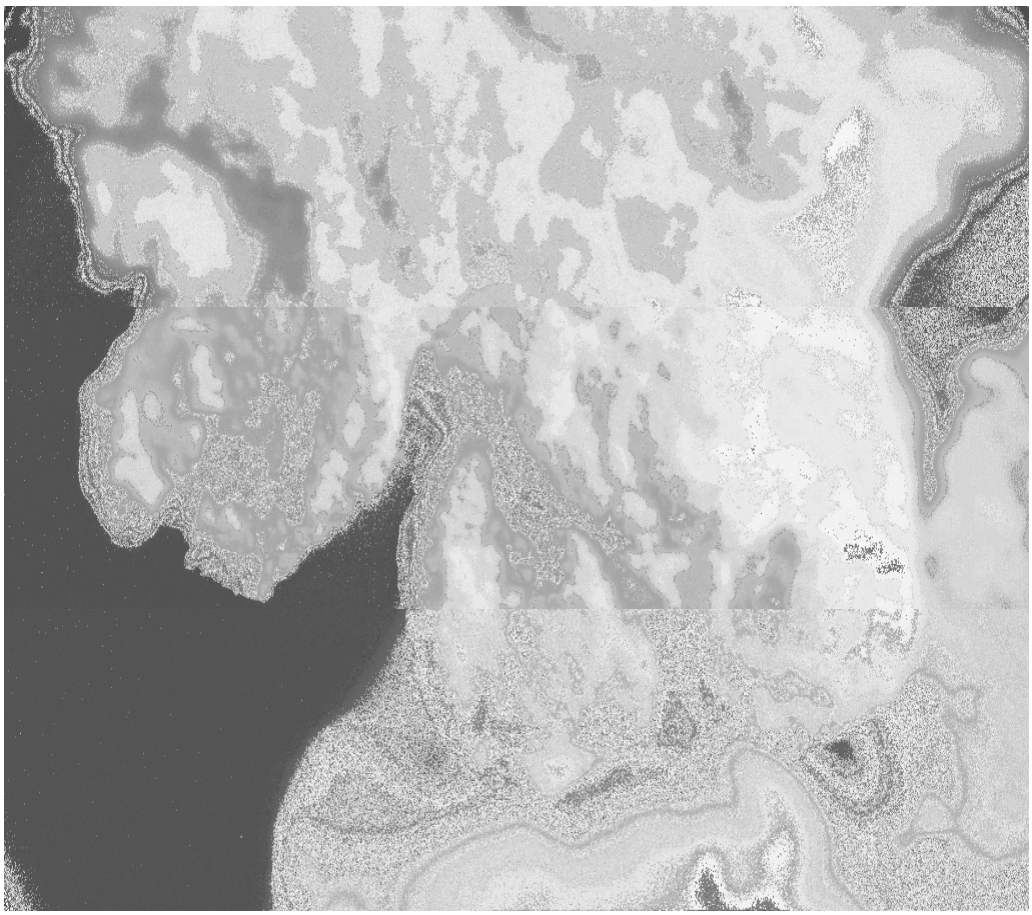

Figure 5.10: Optical micrograph of PE from $[Cr_3O(Cl_3CCO_2)_6.2H_2O]Cl_3CCO_2.3H_2O$ / $AlEt_2Cl$ catalytic system.

5.4.2 Fourier Transform Infrared spectroscopy (FTIR)

A representative of the FTIR spectra of polyethylene, produced using the catalytic system $[Cr_3O(Cl_3CCO_2)_6.2H_2O]Cl_3CCO_2.3H_2O$ / $AlEt_2Cl$ is shown in Figure 5.11. Typically there are six major bands. The two strong peaks, at around 2915 cm^{-1} and 2848 cm^{-1}, are respectively characteristic of C-H asymmetric and symmetric stretching modes. The double medium bands at 1473 cm^{-1} and 1463 cm^{-1} are due to the CH_2 deformation and CH_3 symmetric deformation vibrations respectively. In addition, the doublet band around 730 cm^{-1} and 718 cm^{-1} is due to the CH_2 rocking mode.

There were no significant changes in the FTIR spectrum of PE when the initial monomer pressure varied. Table 5.2 recapitulates the characteristic bands observed in the FTIR spectra of polyethylene produced at various initial monomer pressures. In addition, the relative proportions of crystalline and amorphous portions of PE were measured using the absorption frequencies at 730 cm^{-1} and 720 cm^{-1} as shown in Table 5.3. The ratio of the absorbance at 730 cm^{-1} and 720 cm^{-1} is high. This indicates that PE samples were of high crystallinity.

Table 5.2: Band assignments for FTIR spectra of polyethylene produced at various initial monomer pressures using $[Cr_3O(Cl_3CCO_2)_6.2H_2O]Cl_3CCO_2.3H_2O$ / $AlEt_2Cl$ catalytic system

Assigned PE vibration mode		Initial monomer pressure (kPa)				
		317	412	505	672	795
CH_2 – Stretching	Asymmetric	2916 s	2915 s	2915 s	2916 s	2915 s
	Symmetric	2849 s	2849 s	2849 s	2849 s	2848 s
CH_2 – deformation		1473 m	1473 m	1472 m	1473 m	1473 m
CH_3 – symmetric deformation		1463 m	1463 m	1463 m	1463 m	1463 m
CH_2 – rocking		730 m	730 m	730 m	730 m	730 m
		718 m	718 m	718 m	719 m	718 m

s = strong, m= medium

Table 5.3: Absorbance ratio of polyethylene produced at various initial monomer pressures using $[Cr_3O(Cl_3CCO_2)_6.2H_2O]Cl_3CCO_2.3H_2O$ / $AlEt_2Cl$ catalytic system

Max P_i (kpa)	Intensity (cm^{-1})		A_{730} / A_{719}
	A_{730}	A_{719}	
317	0.08	0.15	0.53
412	0.06	0.21	0.29
505	0.08	0.14	0.57
672	0.06	0.15	0.40
795	0.09	0.17	0.53

Where Max P_i is the maximum initial monomer pressure, A_{730} and A_{720} are the absorption frequencies at 730 cm^{-1} and 720 cm^{-1} respectively.

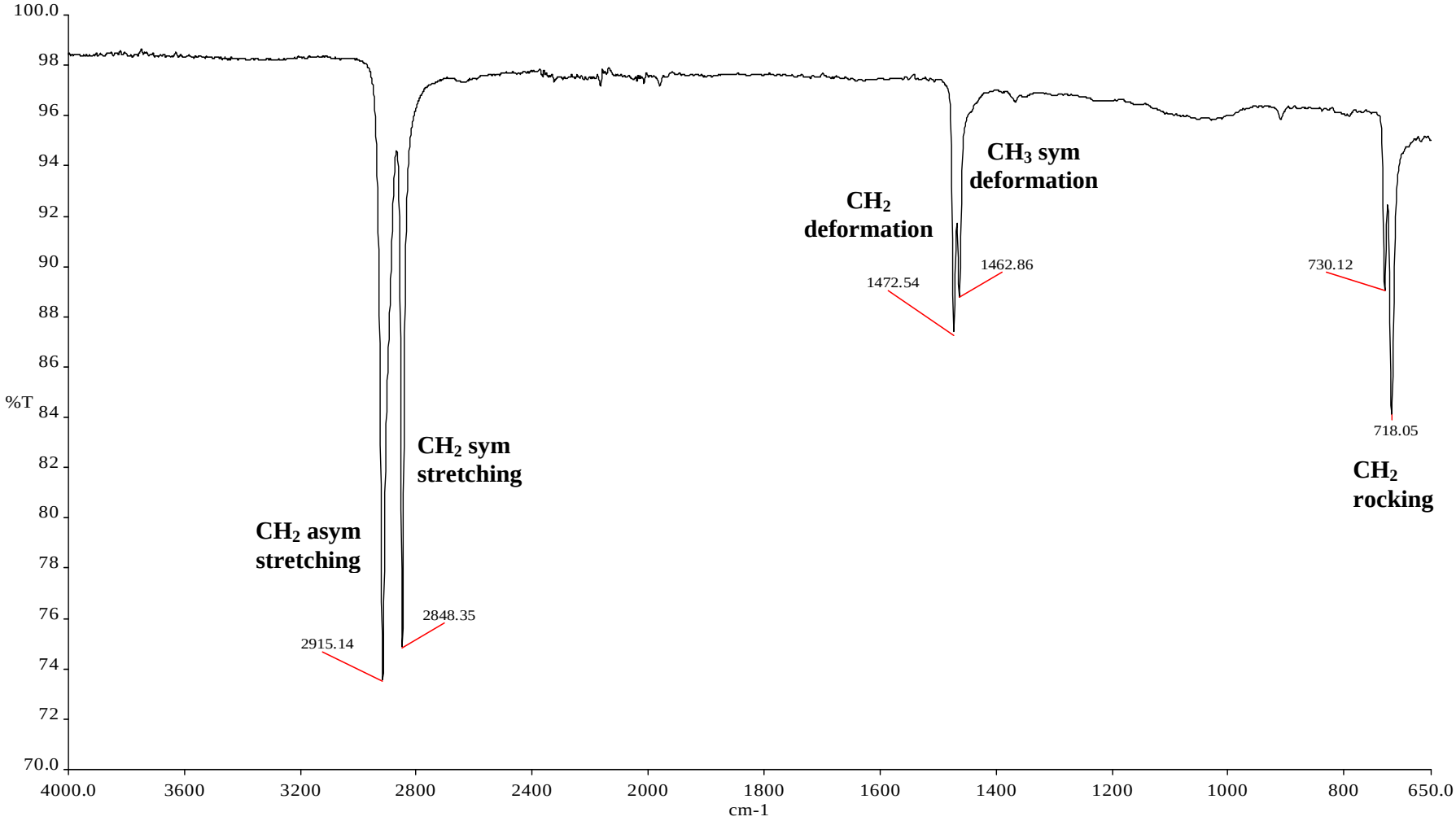

Figure 5.11: A representative FTIR spectrum of polyethylene produced using $[Cr_3O(Cl_3CCO_2)_6.2H_2O]Cl_3CCO_2.3H_2O$ / $AlEt_2Cl$ catalytic system.

5.4.3 Thermal Gravimetric analysis (TGA)

A representative of the TGA curves of PE samples produced using the catalytic system, $[Cr_3O(Cl_3CCO_2)_6.2H_2O]Cl_3CCO_2.3H_2O$ / $AlEt_2Cl$ is shown in Figure 5.12. As seen, the polymer starts decomposing at around 400 ^oC. In addition, 96 % of PE decomposes without any break. This indicates that the polymer is of high purity.

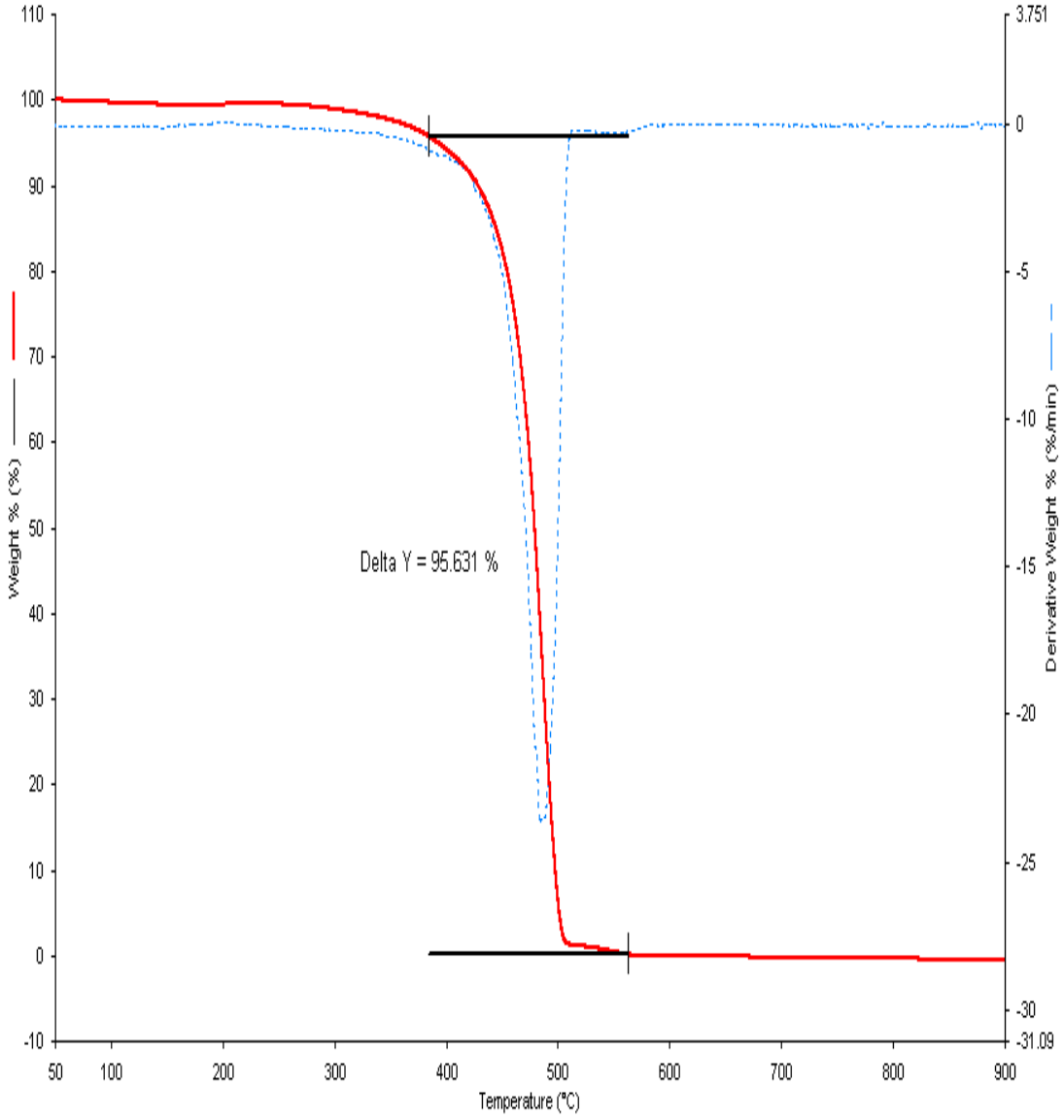

Figure 5.12: A representative thermogram for the decomposition of polyethylene produced using $[Cr_3O(Cl_3CCO_2)_6.2H_2O]Cl_3CCO_2.3H_2O$ / $AlEt_2Cl$ catalytic system.

5.4.4 Differential Scanning Calorimetry (DSC)

DSC measurements of polyethylene samples produced from $[Cr_3O(Cl_3CCO_2)_6.2H_2O]Cl_3CCO_2.3H_2O$ / $AlEt_2Cl$ catalytic system were measured. To study the effect of various initial monomer pressures, the PE samples used for the measurements were produced using five different starting monomer pressures. Their DSC data as well as the crystallinity (X_c) in the polyethylene matrices are summarized in Table 5.4. The degree of crystallinity was estimated by comparing the measured melting enthalpy (from the second scan) to that of a pure polyethylene crystal (289 J/mol) [7, 8]. In addition, the DSC curve of a representative PE sample is shown in Figure 5.13 (direct scan), Figure 5.14 (cooling) and Figure 5.15 (rescanning).

All PE samples show well defined endothermic and exothermic peaks, respectively characteristic of melting and crystallization (Table 5.4). The melting temperatures (142 to 147 ^oC) in the direct scan are found to decrease (136 to 143 ^oC) after annealing and rescanning. In addition, the melting temperatures (T_m) increase with increase in monomer pressure. However, varying the ethylene pressures has little effect on the crystallization temperature. The higher percentage of crystallinity (58.28%) is observed for a PE sample produced with ethylene pressure of 505 kPa and the lower percentage of crystallinity is for a PE sample obtained at 412 kPa. This implies that the percentage of crystallinity is independent of the initial monomer pressure.

Table 5.4: DSC data for polyethylene produced at various initial monomer pressures using $[Cr_3O(Cl_3CCO_2)_6.2H_2O]Cl_3CCO_2.3H_2O$ / $AlEt_2Cl$ catalytic system

P_i (kPa)	1st scan			Crystallization		2nd scan			X_c (%)
	T_m (^oC)	T_o (^oC)	ΔH (J/g)	T_c (^oC)	- ΔH (J/g)	T_m (^oC)	T_o (^oC)	ΔH (J/g)	
317	141.82	128.17	203.04	114.98	153.20	136.08	122.89	158.21	54.74
412	144.51	132.68	87.34	115.61	78.77	136.59	124.45	80.78	27.95
505	146.20	136.42	202.69	113.40	161.40	139.31	125.84	168.42	58.28
672	146.64	134.80	130.08	114.14	102.77	140.41	126.12	106.30	36.78
795	146.03	131.59	172.08	113.07	114.53	142.47	125.45	150.92	52.22

Where

P_i is the maximum initial monomer pressure, T_m, the melting temperature, T_o, the onset temperature, T_c, the crystallization temperature, ΔH, the enthalpy of fusion and X_c is the percentage of crystallinity in the PE samples.

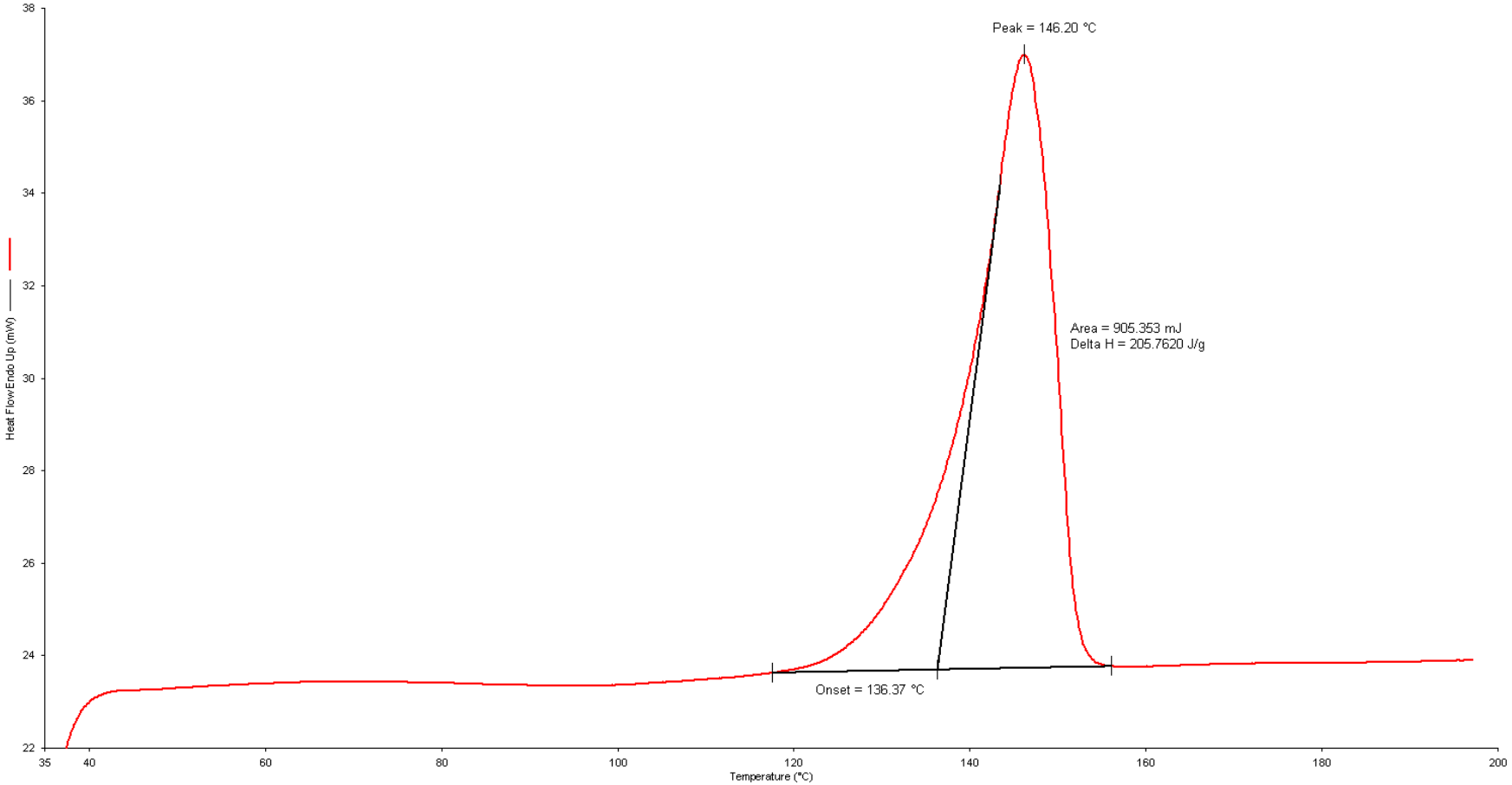

Figure 5.13: A representative DSC first scan of polyethylene produced using $[Cr_3O(Cl_3CCO_2)_6.2H_2O]Cl_3CCO_2.3H_2O$ / $AlEt_2Cl$ catalytic system

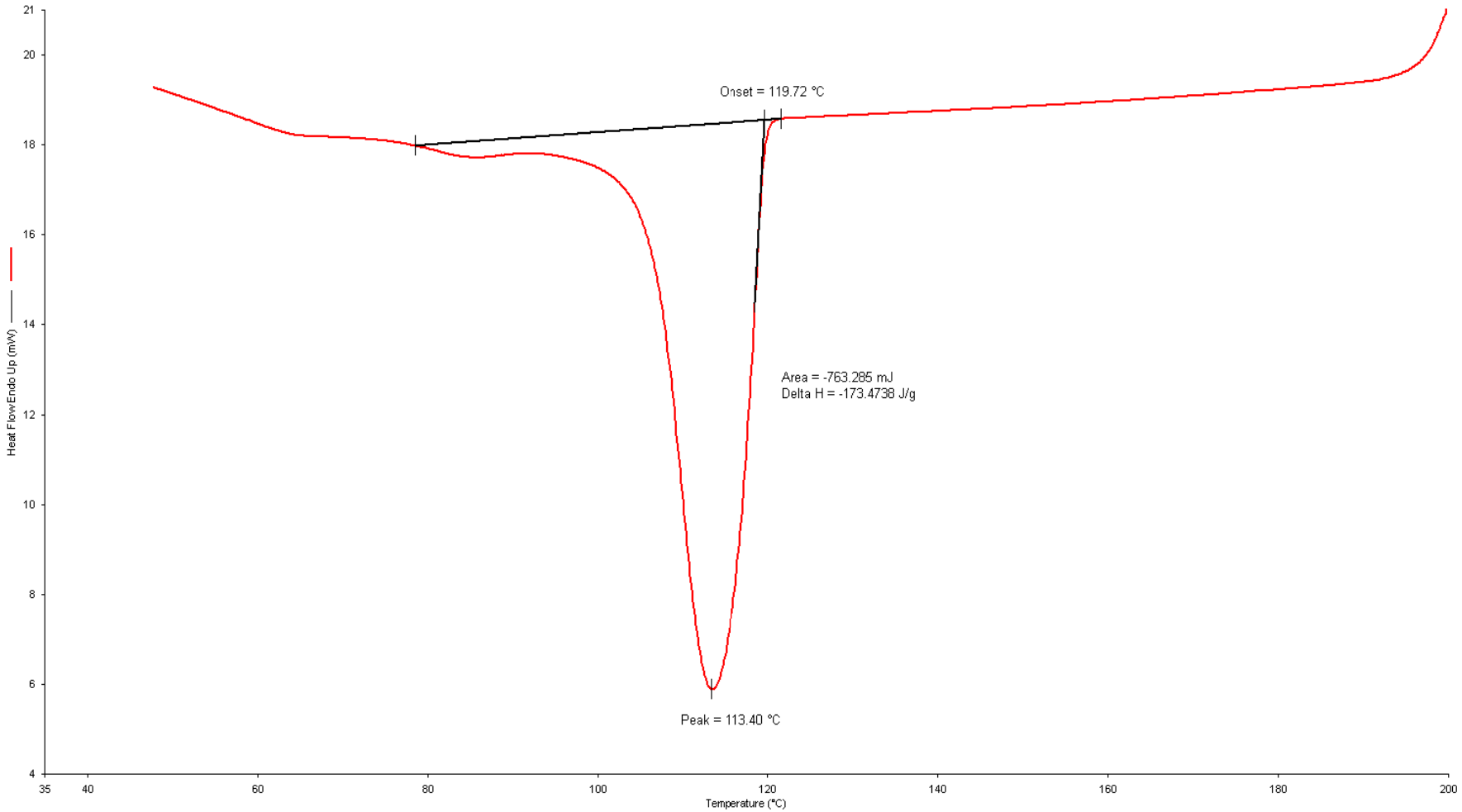

Figure 5.14: A representative DSC cooling scan of polyethylene produced using $[[Cr_3O(Cl_3CCO_2)_6.2H_2O]Cl_3CCO_2.3H_2O$ / $AlEt_2Cl$ catalytic system.

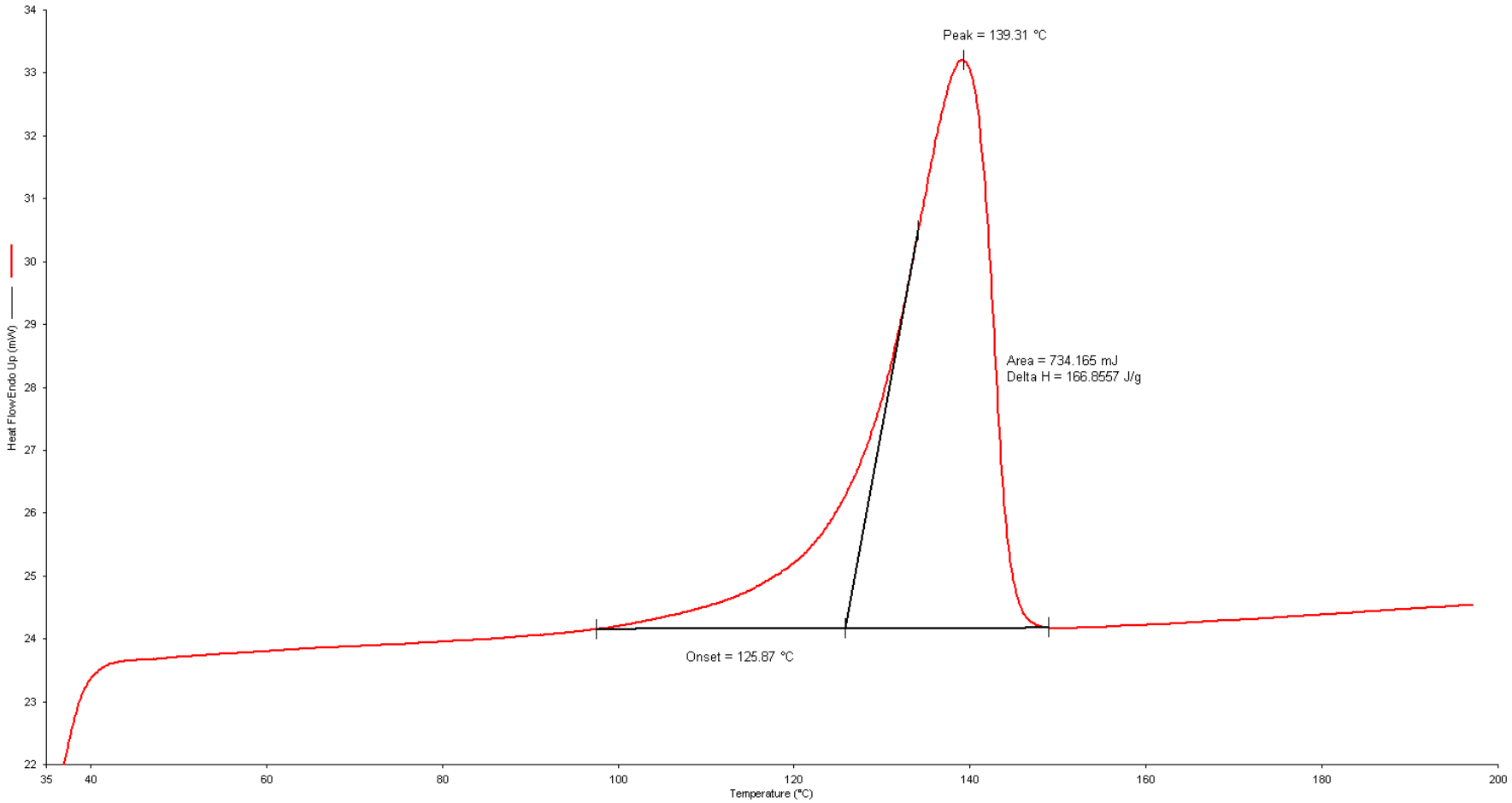

Figure 5.15: A representative DSC rescanning of polyethylene produced using $[Cr_3O(Cl_3CCO_2)_6.2H_2O]Cl_3CCO_2.3H_2O$ / $AlEt_2Cl$ catalytic system.

5.4.5 Hardness

Hardness values of polyethylene produced at various monomer pressures using the $[Cr_3O(Cl_3CCO_2)_6.2H_2O]Cl_3CCO_2.3H_2O$ / $AlEt_2Cl$ catalytic system, were in the range of 50.1 to 59.3 Shore D (Table 5.5). As can be observed, hardness values are independent of the ethylene pressure. This agrees well with the crystallinity values from DSC measurements (X_c). Whereby, hardness values increase with increasing in X_c.

Table 5.5: Hardness data of PE samples produced at constant Al / Cr ratio and variable initial monomer pressures.

P_i (kPa)	T_m (^oC)	X_c (%)	Hardness (Shore D)
317	136.08	54.74	53.1
412	136.59	27.95	50.1
505	139.31	58.28	59.3
672	140.41	36.78	50.3
795	142.47	52.22	51.9

X_c is the crystallinity estimated from the DSC data [8], P_i is the maximum initial monomer pressure and T_m is the melting temperature of the sample.

5.4.6 Density

The proportion of crystals within the mass (density), ρ, of the produced PE was measured as previously detailed in Section 4.5.6. Table 5.6 summarizes the density data obtained and the percentage of crystallinity derived from the density [9, 10]. As expected, the density of PE samples increases as hardness and crystallinity increase. This is due to a higher degree of molecular ordering in PE with high crystallinity. The percentage of crystallinity, calculated from the density value is slightly higher than those from DSC data. This is because the samples were hot pressed, and cooled for one day, at room temperature prior to the density test. This long annealing time, probably reorders the polyethylene molecule better than in DSC measurements (10 minutes annealing).

Table 5.6: Density data of PE samples produced at constant Al / Cr ratio and variable initial monomer pressures; and the comparison of degree of crystallinity obtained from DSC and density results

P_i (kPa)	T_m (^oC)	Hardness (Shore D)	ρ ($g.cm^{-3}$)	X_c^1 (%)	W_c^2 (%)
317	136.08	53.1	0.9328	54.74	55.10
412	136.59	50.1	0.8989	27.95	31.40
505	139.31	59.3	0.9406	58.28	60.56
672	140.41	50.3	0.9079	36.78	37.69
795	142.47	51.9	0.9301	52.22	53.22

X_c^1 is the crystallinity estimated from the DSC data
W_c^2 is the crystallinity calculated with the density value according to equation (1)

5.4.7 Dynamic Mechanical Analysis (DMA)

DMA analysis of a series of different samples has been used to investigate the relaxation behaviors of the polymer using dynamic mechanical parameters such as storage modulus, stiffness, loss modulus, tan δ and complex viscosity. In addition the variations of the dynamic mechanical properties as a function of temperature are presented in Figures 5.16 to 5.20.

The storage modulus, stiffness and complex viscosity curves are similar. They decrease with increasing temperature. This is because their chain movement increases with heat [11].

Damping spectra show a γ-peak of the principal relaxation (~ -120 ^{o}C) at the glass transition temperature [12-14]; a relaxation β-peak (- 30 ^{o}C $\leq$ β-T_g $\leq$ 15 ^{o}C), attributed to local motions in the amorphous phase [15] and an α-peak (~ 40 ^{o}C) attributed to the relaxation in crystalline parts of the PE [16-19]. These peaks correspond to drops of the storage modulus, which increases at low temperatures with increase in crystallinity. PE samples with higher percentage of crystallinity show an increase in their γ and α peaks. In addition, their T_g is observed to shift to higher temperature. The β-T_g peak is not completely resolved in samples with higher crystallinity.

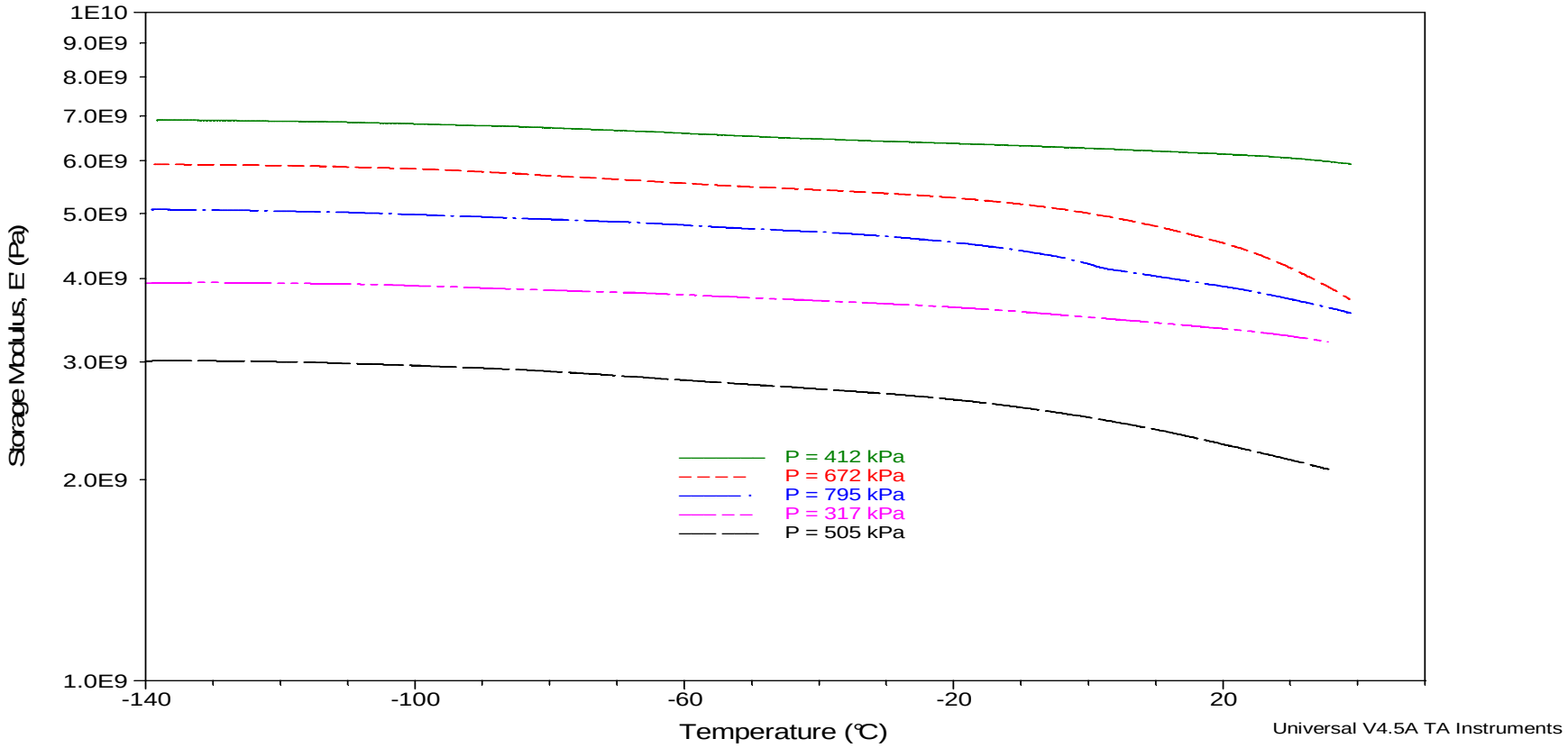

Figure 5.16: Effect of temperature on storage modulus of PE samples produced at various initial monomer pressures using $[Cr_3O(Cl_3CCO_2)_6.2H_2O]Cl_3CCO_2.3H_2O$ / $AlEt_2Cl$ catalytic system

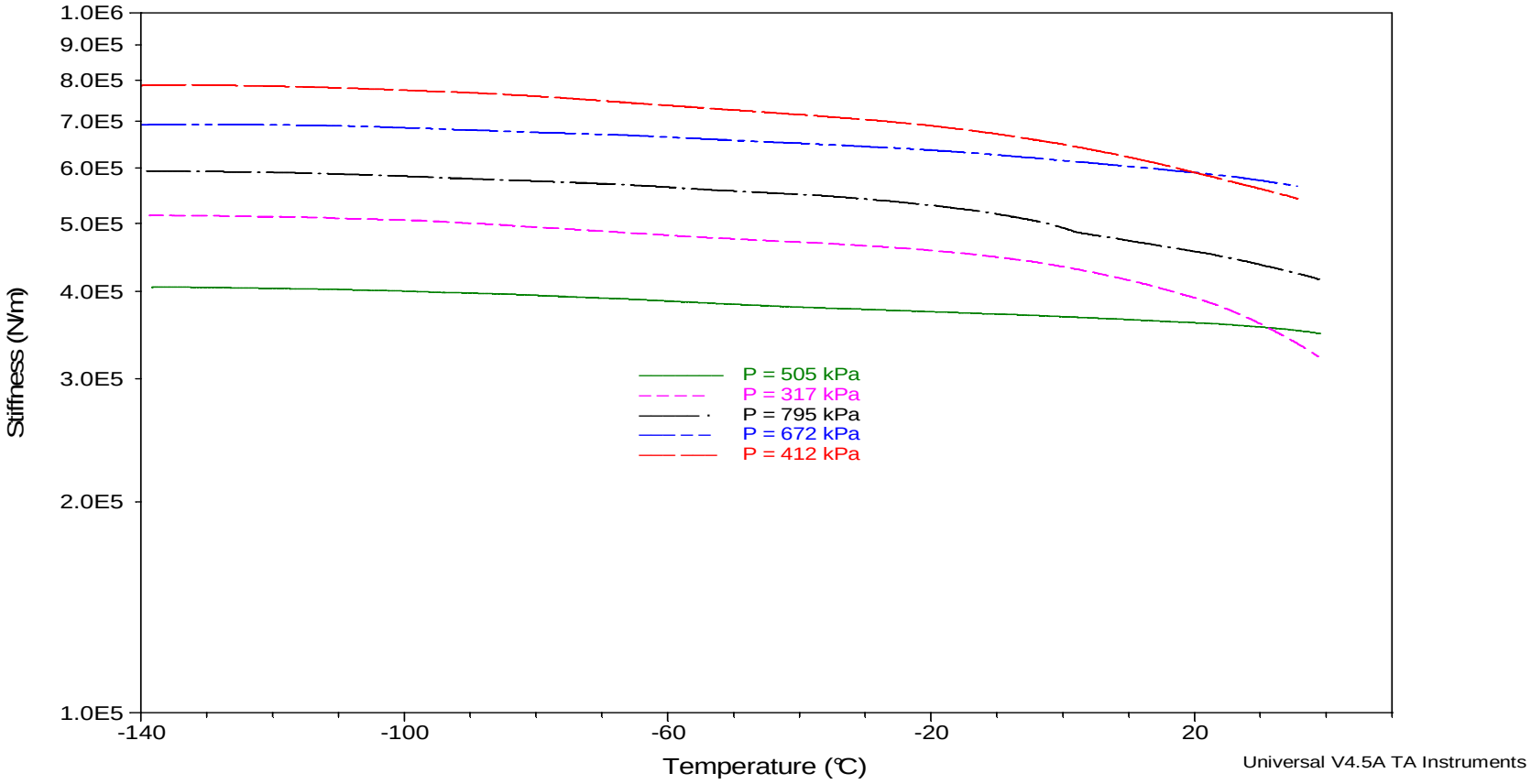

Figure 5.17: Effect of temperature on stiffness of PE samples produced at various initial monomer pressures using $[Cr_3O(Cl_3CCO_2)_6.2H_2O]Cl_3CCO_2.3H_2O$ / $AlEt_2Cl$ catalytic system

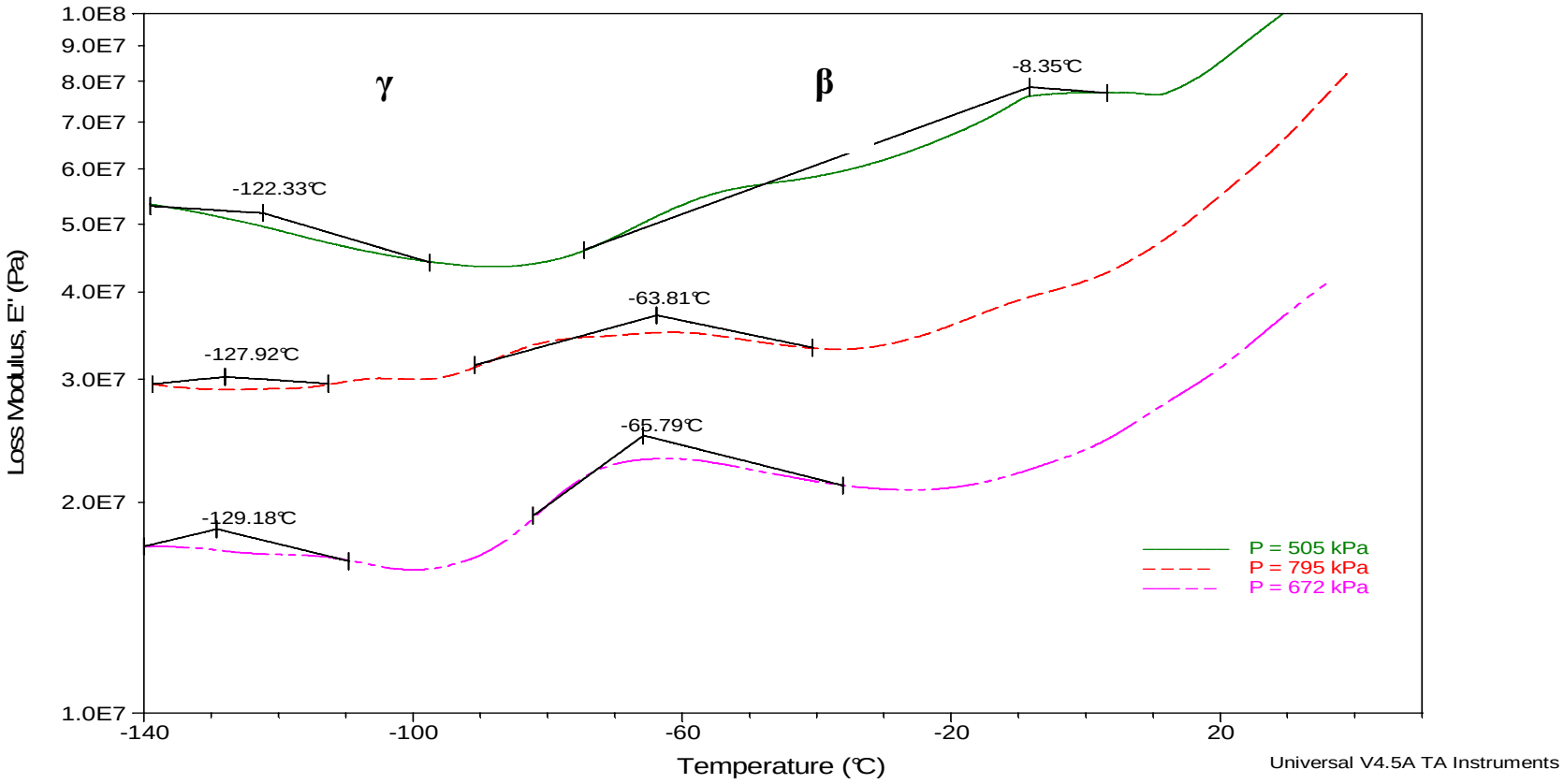

Figure 5.18: Effect of temperature on loss modulus of PE samples produced at various initial monomer pressures using $[Cr_3O(Cl_3CCO_2)_6.2H_2O]Cl_3CCO_2.3H_2O$ / $AlEt_2Cl$ catalytic system

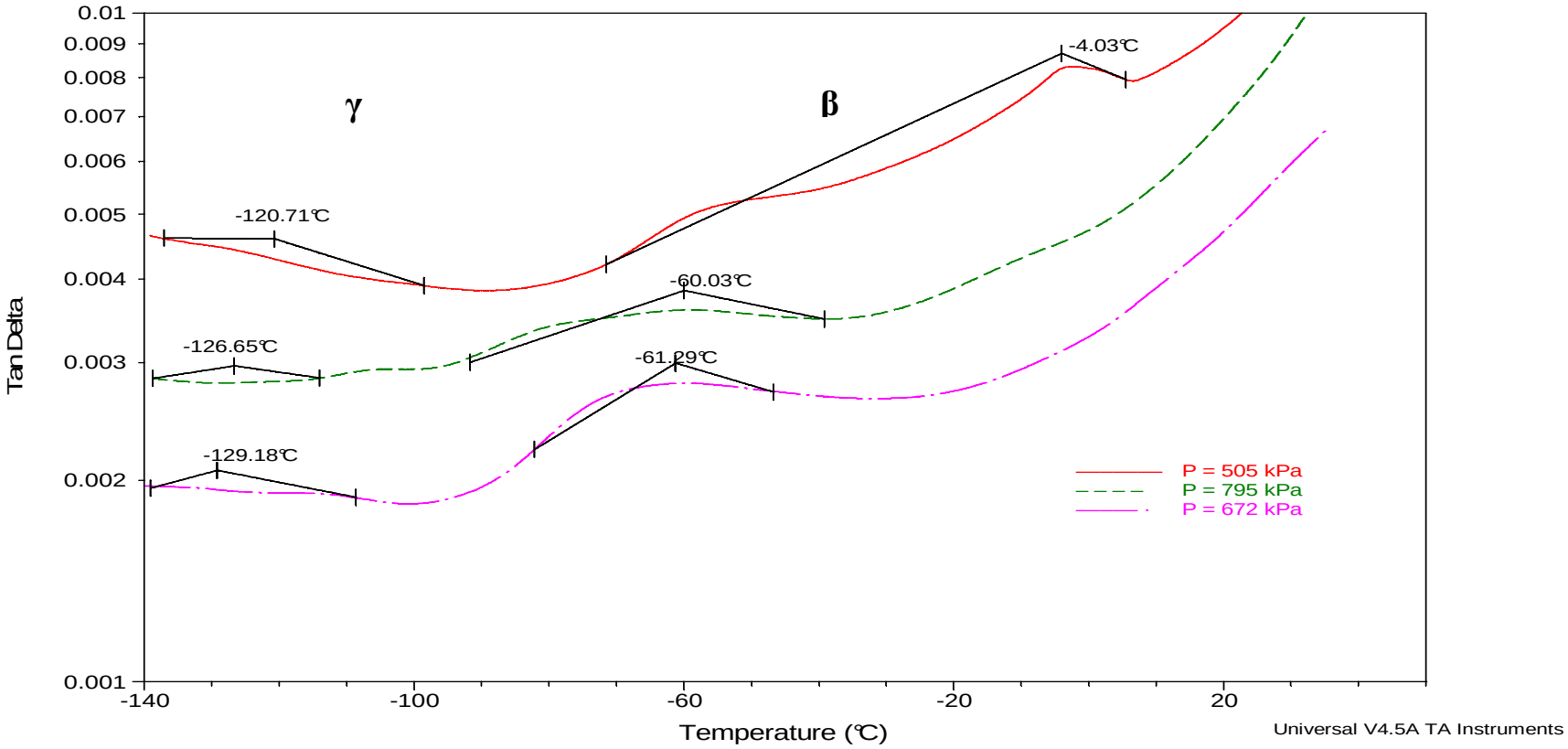

Figure 5.19: Effect of temperature on Tan Delta of PE samples produced at various initial monomer pressures using $[Cr_3O(Cl_3CCO_2)_6.2H_2O]Cl_3CCO_2.3H_2O$ / $AlEt_2Cl$ catalytic system

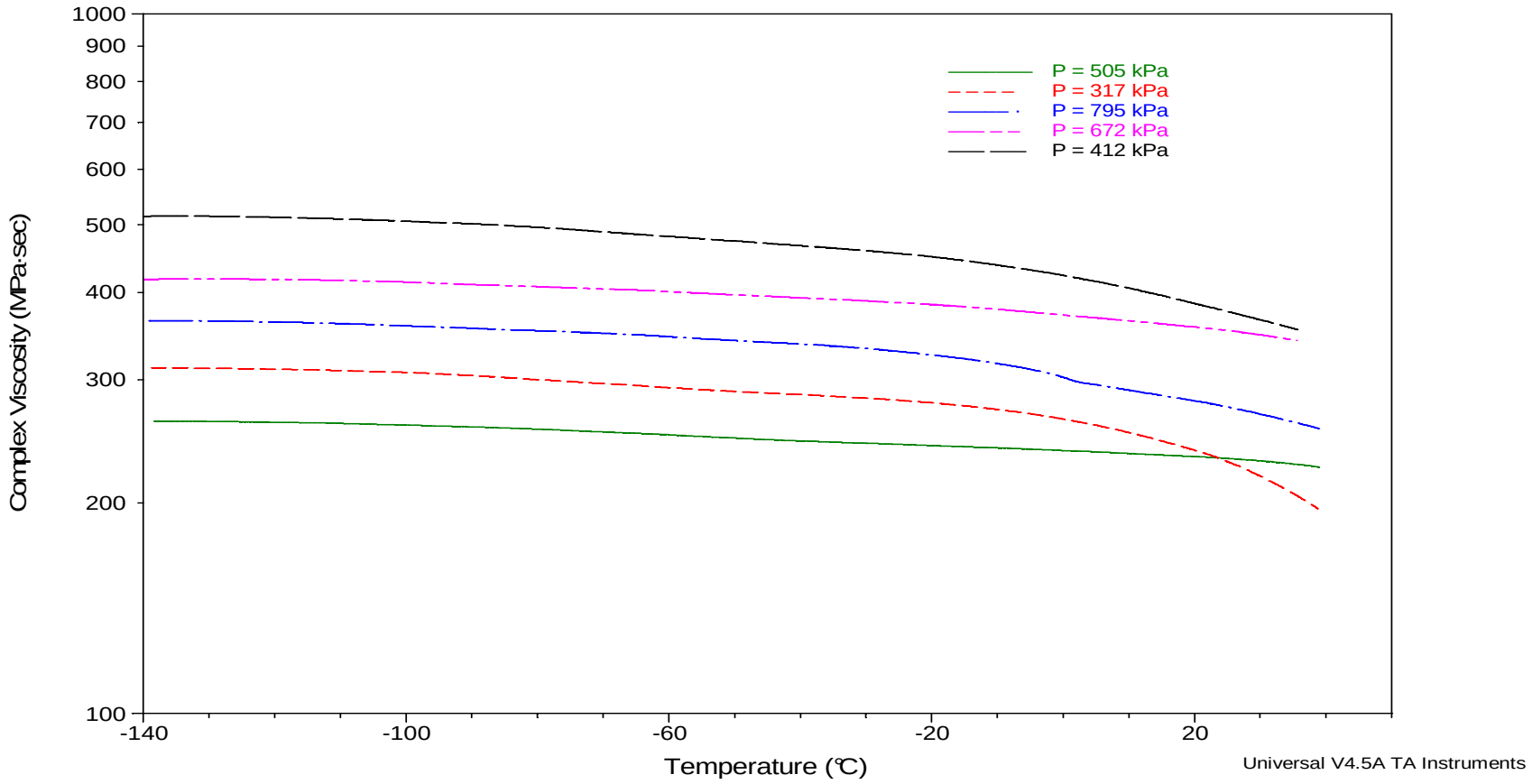

Figure5.20: Effect of temperature on the complex viscosity of PE samples produced at various initial monomer pressure susing $[Cr_3O(Cl_3CCO_2)_6.2H_2O]Cl_3CCO_2.3H_2O$ / $AlEt_2Cl$ catalytic system

5.4.8 Nuclear magnetic resonance spectroscopy (NMR)

High temperature ^{1}H and ^{13}C NMR analyses of all PE samples, produced at various initial monomer pressures using the $[Cr_3O(Cl_3CCO_2)_6.2H_2O]Cl_3CCO_2.3H_2O$ / $AlEt_2Cl$ catalytic system, were carried out. Their ^{1}H and ^{13}C NMR spectra presented in Figures 5.21 and 5.22 show single peaks at around 1.3 and 30 ppm respectively. This closely resembles NMR data for ultrahigh molecular weight polyethylene (UHMWPE) [20, 21].

5.5 Conclusion

The trinuclear oxo-centered, $[Cr_3O(Cl_3CCO_2)_6.2H_2O]Cl_3CCO_2.3H_2O$ in combination with $AlEt_2Cl$ shows high activity in the homopolymerization of ethylene at 40 ^{o}C. The polymerization reaction is influenced by the monomer pressure. In addition, the polymers produced have high melting point, density and crystallinity.

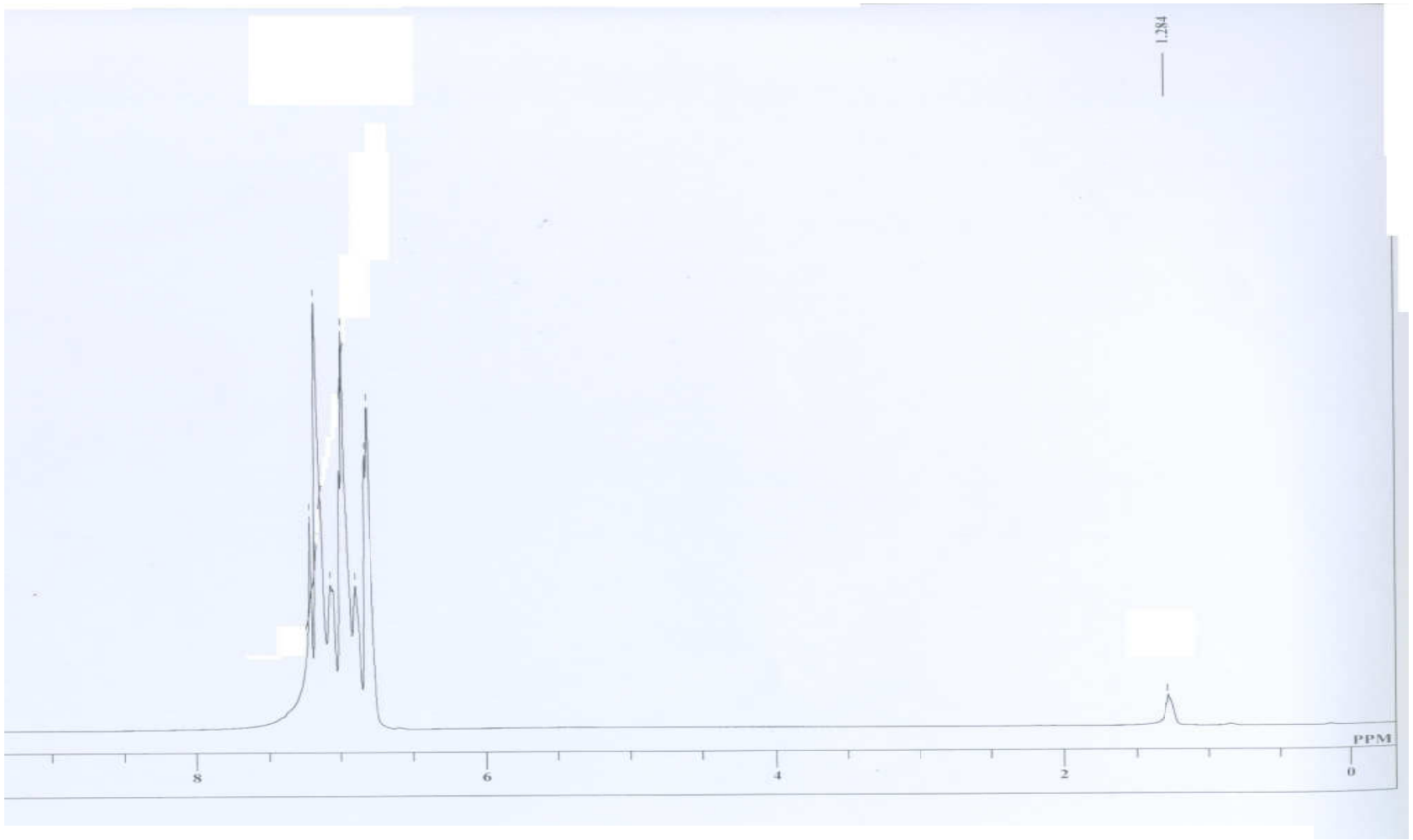

Figure 5.21: ^{1}H- NMR spectra obtained from PE samples produced using $[Cr_3O(Cl_3CCO_2)_6.2H_2O]Cl_3CCO_2.3H_2O$ / $AlEt_2Cl$ catalytic system

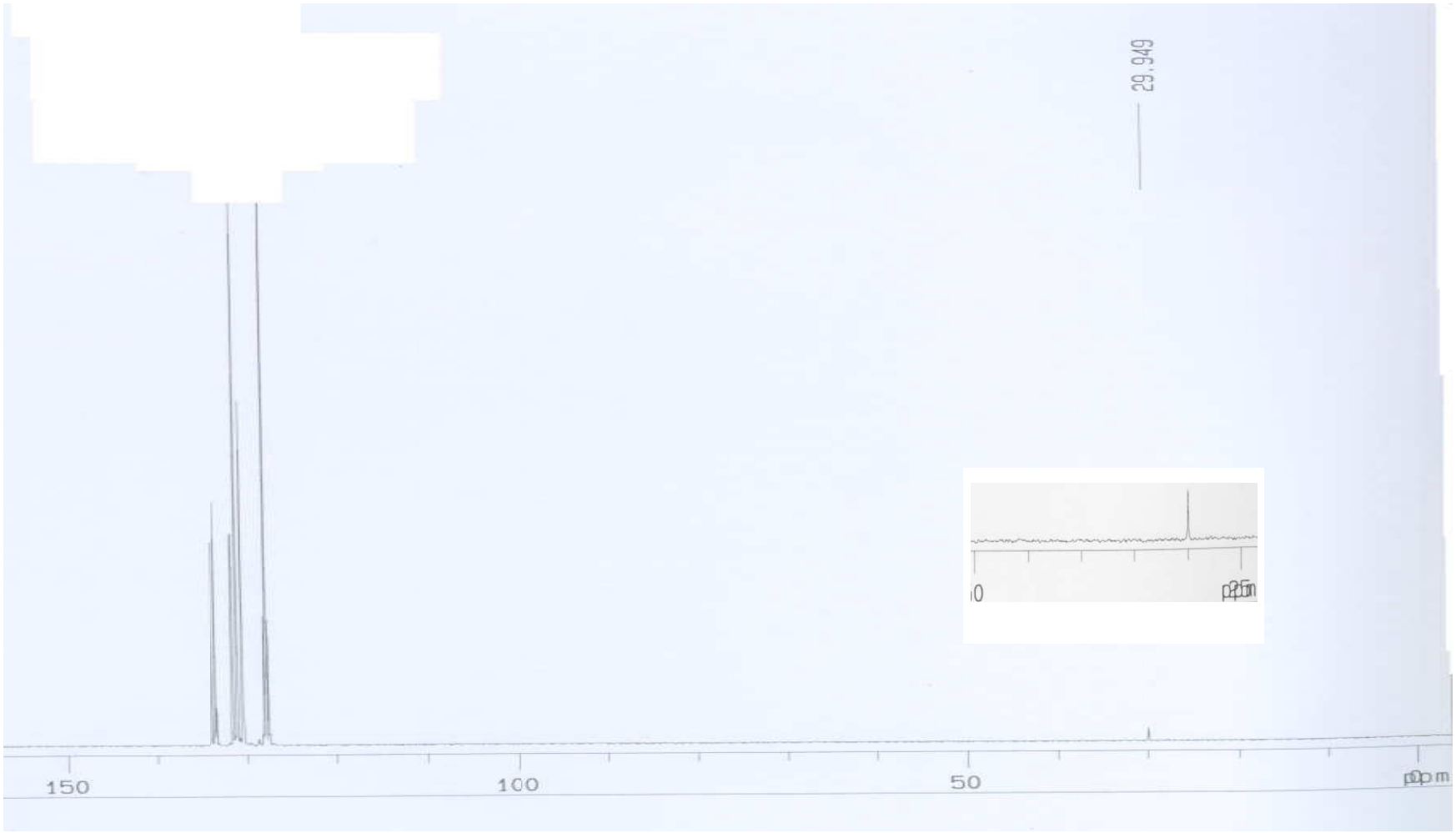

Figure 5.22: ^{13}C- NMR spectra obtained from PE samples produced using $[Cr_3O(Cl_3CCO_2)_6.2H_2O]Cl_3CCO_2.3H_2O$ / $AlEt_2Cl$ catalytic system

5.6 References

1. B. B. Mougang D. Soume, Rosiyah Yahya, Seng Neon Gan and Seik Weng Ng, Acta Cryst. **E64**, m1175 (2008).
2. S. N. Gan, A. M. Jelan and C. P. Ooi, (2000) Trinuclear oxo-centered chromium(III) carboxylate complexes as Ziegler-Natta catalysts for ethylene polymerization in Progress and Development of Catalytic Olefins Polymerization, edited by T. Sano, T. Uozumi, H. Nakatami & M. Terano, 25-32, Tokyo: Technology and Education Publishers.
3. C.P. Ooi, Master thesis, University of Malaya, Kuala Lumpur, 1996.
4. T. Keii, K. Soga and N. Saiki, J. Polym. Sci., **C16**, 1507 (1967).
5. B. V. Kokta and R. G. Raj, Polym. Bull., **22**, 103-110 (1989).
6. L. C. S. Maria and F. M. B. Coutinho, Polym. Bull., **29**, 193-198 (1992).
7. L. H. Sperling, "Introduction to Physical Polymer Science", J. Wiley & sons., Inc.. 328 (1992).
8. X. Xu, J. Xu, K. Feng, W. Chen, J. Appl. Polym. Sci., **77**, 1709-1715 (2000).
9. A. Min Min, T. G. Chuah and T. R. Chantara, Material and Design, **29**, 992 – 999 (2008)
10. P. J. Sinko and A. N. Martin, "Martin's physical pharmacy and pharmaceutical sciences", fifth edition, 606 – 607 (2005).
11. K. Menard, Dynamic Mechanical Analysis: a practical introduction, CRC Press LLC, USA, (1999).
12. A. H. Willbourne, Trans. Faraday Soc., **54**, 717 (1958).
13. T. F. Schatzki, J. Polym. Sci. **57**, 337 (1962).
14. R. F. Boyer, Rubber Chem. Technol., **34**, 01303 (1963).
15. J. V. Gulmine and L. Akcelrud, Eur. Polym. J., **42,** 553 (2006).

16. A. Pegoretti, M. Ashkar, C. Migliaresi, G. Marom, Comos. Sci. Technol., **60**, 1181 – 1189 (2000).
17. N. Alberola, J. Y. Cavaille and J. Perez, J. Polym., Sci. (B), Polym Phys. Ed., **28**, 569 (1990).
18. R. Popli, M. Glotin, L. Manderlkern, J. Polym. Sci. Polym. Phys. Ed., **22**, 407 (1984).
19. R. H. Boyd, Polymer, **26**, 1123 (1985).
20. A. Kaji, Y. Akimoto and M. Murano, J. Polym. Sci. (A) Polym. Chem., 29, 1987 (1991).
21. A. J. Brandolini, D. D. Hills, "NMR Spectra of Polymers and Polymer Additives" New York, Marcel Dekker, (2000).